Article
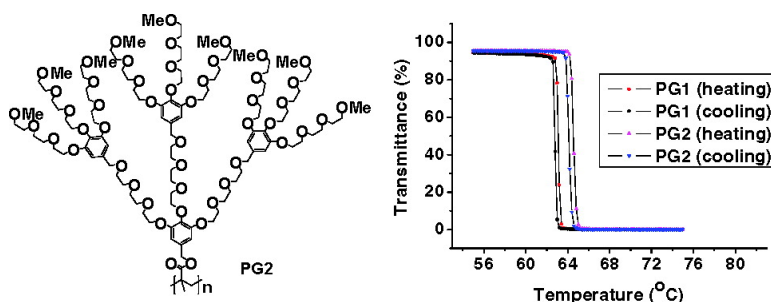
Thermoresponsive Dendronized Polymers

Wen Li, Afang Zhang, Kirill Feldman, Peter Walde, and A. Dieter Schlu#ter

More About This Article

Additional resources and features associated with this article are available within the HTML version:

- Supporting Information
- Links to the 1 articles that cite this article, as of the time of this article download
- Access to high resolution figures
- Links to articles and content related to this article
- Copyright permission to reproduce figures and/or text from this article

View the Full Text HTML

Thermoresponsive Dendronized Polymers

Wen Li,[†] Afang Zhang,*[,†,‡] Kirill Feldman,[†] Peter Walde,[†] and A. Dieter Schlüter[†]

Institute of Polymers, Department of Materials, ETH Zurich, Wolfgang-Pauli-Strasse 10, HCI G525, 8093 Zurich, Switzerland, and School of Materials Science and Engineering, Zhengzhou University, Daxue Beilu 75, Zhengzhou 450052, China

Received January 18, 2008; Revised Manuscript Received March 26, 2008

ABSTRACT: The efficient synthesis of high molar mass, first- (**G1**) and second-generation (**G2**) dendronized polymethacrylate derivatives **PG1** and **PG2**, respectively, and their thermoresponsive properties in aqueous solution are described. All dendrons are branched 3-fold and were synthesized on the multigram scale using gallic acid as branching point and tri(ethylene glycol) (TEG) units as linker. The corresponding macromonomers carry methoxy groups in the periphery and are water-soluble, which allows polymerizing in aqueous medium. For comparison, **PG1** and **PG2** were also prepared in DMF solution and in bulk. These polymers are fully soluble in water at room temperature and turn turbid at elevated temperatures (approximately 62−65 °C), a phenomenon that is typically referred to as thermoresponsiveness. This phase transition was investigated by ^{1}H NMR spectroscopy and turbidity measurements using UV/vis spectroscopy. The effect of molar mass and concentration on this transition was examined. In accordance with the normal usage, this transition temperature is referred to as lower critical solution temperature (LCST). Aggregates with sizes in the range of a few micrometers were observed above the LCSTs by conventional optical microscopy. Finally, the thermally induced aggregation and deaggregation processes were video-taped in high resolution.

Introduction

Thermoresponsive polymers have drawn considerable interest[1] and are being investigated for promising applications.[2] In aqueous solution, these polymers collapse above their lower critical solution temperature (LCST)[3] because of dehydration of the polymer chains, and subsequently form aggregates. The processes of dehydration and aggregation have been investigated by techniques including ^{1}H NMR and dielectric relaxation spectroscopy as well as turbidimetry and dynamic light scattering. Because of their biocompatibility, polyethylene glycol (PEG) and poly(*N*-isopropylacrylamide) (P*N*iPAM) are the most often investigated thermoresponsive polymers. They show LCSTs above 100 °C and around 32 °C, respectively. Their heating transitions tend to be sharp, whereas upon cooling, considerable hystereses are often observed. These overall broad transitions tend to be disadvantageous for applications. Therefore, developing novel thermoresponsive polymers with fast transitions in both directions remains an important challenge. The structural motifs of PEG and P*N*iPAM have been incorporated into more complex (hybrid) polymers comprised of those thermoresponsive and also nonresponsive structural elements in a variety of different arrangements. Most of these hybrid systems are linear block copolymers, e.g., where one block is PEG, oligoethylene glycol (OEG), or P*N*iPAM,[4] though recently, interest has also been paid to nonlinear congeners.[5] As one may have intuitively suggested, not only the ratio between hydrophilic and hydrophobic units[6] determines the responsiveness of the hybrid polymers but also how the responsive units are incorporated. Such architecture effects have attracted more and more attention.[7] For example, polymers containing OEG blocks or those grafted with OEG units show quite different thermoresponsiveness with LCSTs ranging for both cases from approximately 25 to 80 °C.[8] Also random copolymers with repeat units differing in their hydrophilicity exhibit rather different LCSTs. This was shown for copolymers made from hydrophobic 2-(2-methoxyethoxy)ethyl methacrylate and hydrophilic OEG methacrylate, which, as an additional interesting feature, exhibit quite sharp thermal transitions (3−4°).[9]

Much attention has also been paid to developing novel thermoresponsive polymers on the basis of dendrimers and hyperbranched polymers. Most of them were constructed by attaching thermoresponsive units to the "surface" of these dendritic macromolecules.[10] Additionally, there are a few reports on branched macromolecules constructed from hydrophilic and hydrophobic units such that the overall hydrophilicity−hydrophobicity balance renders them thermoresponsive.[11] For certain dendrimers whose hydrophilicity increases with generation, it was found that LCST decreases.[10d,i] This seemingly astounding finding was rationalized in terms of densely packed structures, which facilitate the dehydration process (impact of steric hindrance on LCST). For example, isobutyramide-terminated PAMAM dendrimers of generation G1 to G3 showed LCSTs of 76, 60, and 42 °C, respectively. For hyperbranched polymers, the LCSTs are dependent on the overall hydrophilicity−hydrophobicity balance and on molar mass.[11c,d]

Dendronized polymers are a class of nanoscopic, rigid polymers with pendant dendrons at each repeating unit.[12] Because of their chemical structure comprising a linear backbone surrounded by a dense layer of monodisperse, regularly branched units, it was an important question to explore in so much as such polymers could eventually be used to create an unprecedented thermoresponsive behavior based on this unique architecture. Given the considerable sizes of individual dendronized polymers with diameters between 3 and 7 nm and average lengths from a few hundred nanometers up to micrometers, it was suspected that their collapse could give rise to aggregates with sizes large enough to be detected by conventional optical microscopy.[13,14] This would allow for the fascinating option to directly video-monitoring aggregate formation by this simple technique.[10j]

Recently, representatives **PG1(OH)** and **PG2(OH)** with 3-fold branched OEG-based dendrons and free (unprotected) hydroxyl groups in the periphery were reported (Figure 1).[15] Unexpectedly, these dendronized polymers are not thermore-

* Corresponding author. E-mail: zhang@mat.ethz.ch or azhang@zzu.edu.cn. Fax: 41 44-6331390.
† ETH Zurich.
‡ Zhengzhou University.
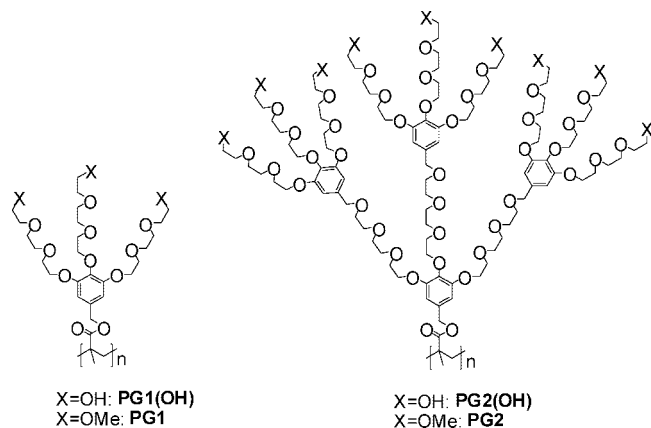
Figure 1. Chemical structures of the hydroxyl- and methoxy-terminated dendronized polymethacrylates **PG1(OH)/PG2(OH)** and **PG1/PG2** synthesized in earlier[15] and the present work, respectively.

sponsive but rather fully water-soluble in various concentrations (0.5−20%) and a broad temperature range (25−80 °C). The present work describes the efficient synthesis of the structurally closely related methoxy-terminated high molar mass polymers **PG1** and **PG2** and shows that this change in the nature of the peripheral groups results in a rather peculiar thermoresponsive behavior with unprecedented sharp transitions across the LCST upon both heating and cooling. It will also be shown that optical microscopy equipped with a CCD camera can be used for a real-time monitoring of the aggregation and deaggregation process of these polymers.

Experimental Section

Materials. Tosylated triethylene glycol monomethyl ether (Me-TEG-Ts) was synthesized according to a literature method.[16] Compound **2d** was synthesized according to our previous report.[15] Azobis(isobutyronitrile) (AIBN) was recrystallized twice from methanol. Tetrahydrofuran (THF) was refluxed over lithium aluminum hydride (LAH) and dichloromethane (DCM) was distilled from CaH$_2$ for drying. Other reagents and solvents were purchased at reagent grade and used without further purification. All reactions were run under a nitrogen atmosphere. Macherey-Nagel precoated TLC plates (silica gel 60 G/UV$_{254}$, 0.25 mm) were used for thin-layer chromatography (TLC) analysis. Silica gel 60 M (Macherey-Nagel, 0.04−0.063 mm, 230−400 mesh) was used as the stationary phase for column chromatography.

Instrumentation and Measurements. ^{1}H and ^{13}C NMR spectra were recorded on Bruker AV 500 (^{1}H: 500 MHz, ^{13}C: 125 MHz) spectrometers, and chemical shifts are reported as δ values (ppm) relative to internal Me$_4$Si. High-resolution MALDI-TOF-MS analyses were performed by the MS service of the Laboratorium für Organische Chemie, ETH Zürich, on IonSpec Ultra instruments. Elemental analyses were performed for the polymer samples **PG1** (Table 1, entry 1) and **PG2** (Table 1, entry 4) by the Mikrolabor of the Laboratorium für Organische Chemie, ETH Zürich. Gel permeation chromatography (GPC) measurements were carried out on a PL-GPC 220 instrument with 2 × PL-Gel Mix-B LS column set (2 × 30 cm) equipped with refractive index (RI), viscosity, and light scattering (LS; 15 and 90° angles) detectors, and DMF (containing 1 g L^{-1} LiBr) as eluent at 45 °C. Universal calibration was performed with poly(methyl methacrylate) standards in the range of M_p = 2680 to 3 900 000 (Polymer Laboratories Ltd., U.K.). Differential scanning calorimetry (DSC) measurements were performed on a DSC Q1000 differential scanning calorimeter from TA Instruments in a temperature range of −80 to +200 °C with a heating rate of 10 °C min^{-1}. Samples of a total weight ranging between 3 and 10 mg were closed into aluminum pans of 40 μL, covered by a holed cap, and analyzed under a nitrogen atmosphere. The glass transition temperature (T_g) was determined in the second

heating run. The AFM measurements were carried out on a Nanoscope IIIa Multi Mode Scanning probe microscope (from Digital Instruments, San Diego, CA) operated in the tapping mode with an "E" scanner (scan range 10 μm × 10 μm) and operated in the tapping mode at room temperature in air. Olympus silicon OMCL-AC160TS cantilevers (from Atomic Force F&E GmbH, Mannheim, Germany) were used with a resonance frequency between 200 and 400 kHz and a spring constant around 42 N/m. The samples were prepared by spin-coating (2000 rpm) the polymer solution (3−4 mg/L chloroform) onto freshly cleaved mica (from PLANO W. Plannet GmbH, Wetzlar, Germany). For the contour length analysis, AFM images were taken with a scan size of 600 nm × 600 nm (corresponding to 512 × 512 pixels). The contour length of individual polymer chains was determined by manually drawing lines with a step length of about 5 nm along the polymer chains using the software Image J (version 1.34s). The error for determination of the chain length is ±2.6% or less when repeated measurements were done on the same polymer chain. UV/vis turbidity measurements were carried out for the lower critical solution temperature (LCST) determination on a Varian Cary 100 Bio UV/vis spectrophotometer equipped with a thermostatically regulated bath. Solutions of the polymers in deionized water (with concentration from 0.05 wt% to 4 wt%) were filtered with a 0.45 μm filter before adding into a cuvette (path length 1 cm), which was placed in the spectrophotometer and heated or cooled at a rate of 0.2 °C min^{-1}. The absorptions of the solution at λ = 500 nm were recorded every minute. Optical micrographs were recorded on a Leica DMRX instrument (objective lens × 50) equipped with a halogen-lamp and a color CCD camera (Leica DFC480) connected to an imaging and processing system. A hot-stage from Mettler (model FP82TM) was used. The polymer solutions (0.25 wt %) were sealed inside a concavity slide, and the aggregation process was recorded every second with heating and cooling rates of 0.5 °C min^{-1}. One of the movies in the Supporting Information was recorded from 50 μL of aqueous solution of **PG1** (Table 1, entry 2) at a concentration of 0.25 wt %, and the heating and cooling program for monitoring the aggregation process is: started from 62 °C with heating rate 0.5 °C·min^{-1} to 64 °C, kept at 64 °C for 1 min, and then cooled at a rate of 0.5 °C min^{-1} to 62 °C. The total recording time is 9 min, and then compressed with Adobe Premiere into 35 s. The other movie in the Supporting Information was recorded from 50 μL of an aqueous solution of **PG2** (Table 1, entry 5) at a concentration 0.25 wt %, and the heating and cooling program for monitoring the aggregation process is as follows: start from 63 °C with a heating rate 0.5 °C min^{-1} to 65 °C, maintain at 65 °C for 1 min, and then cool at a rate of 0.5 °C min^{-1} to 63 °C. The total recording time is 9 min, which was then compressed with Adobe Premiere into 34 s.

Synthesis. *Methyl 3,4,5-Tris(2-(2-(2-methoxyethoxy)ethoxy)-ethoxy)benzoate (2a).* A mixture of methyl gallate (12.04 g, 65.38 mmol), Me-TEG-Ts (83.23 g, 261.5 mmol), KI (8.37 g, 52.30 mmol), and potassium carbonate (K$_2$CO$_3$) (90.36 g, 653.8 mmol) in dry DMF was stirred at 80 °C over 24 h. After removal of DMF in vacuo, the residue was extracted with DCM. The organic phase was washed sequentially with NaHCO$_3$ and brine, and then dried over MgSO$_4$. After filtration, the solvent was evaporated in vacuo. Purification by column chromatography with DCM/MeOH (30:1, v/v) afforded **2a** as a colorless oil (38.40 g, 94%). ^{1}H NMR (CDCl$_3$): δ 3.36 (s, 9H, CH$_3$), 3.52−3.53 (m, 6H, CH$_2$), 3.60−3.65 (m, 12H, CH$_2$), 3.69−3.72 (m, 6H, CH$_2$), 3.78 (t, 2H, CH$_2$), 3.84−3.86 (m, 7H, CH$_2$ + CH$_3$), 4.18 (t, 4H, CH$_2$), 4.20 (t, 2H, CH$_2$), 7.27 (s, 2H, CH). ^{13}C NMR (CDCl$_3$): δ 52.32, 59.17, 68.96, 69.76, 70.67, 70.71, 70.83, 70.97, 72.07, 72.54, 76.95, 77.20, 77.46, 109.11, 125.09, 142.67, 152.43, 166.75. HR-MS: *m/z* calcd, 645.32; found, 645.3094 [M + Na]$^+$.

3,4,5-Tris(2-(2-(2-methoxyethoxy)ethoxy)ethoxy)benzyl alcohol (2b). LAH (3.95 g, 104.1 mmol) was added to a solution of **2a** (32.40 g, 52.03 mmol) in dry THF (300 mL) at −5 °C, the mixture was stirred for 30 min, then warmed to r.t. and stirred for another 3 h. The reaction was quenched by dropwise addition of water (10 mL), 10% NaOH (40 mL), and water (50 mL), successively. The

Table 1. Conditions for and Results of the Polymerization of Macromonomers 2c and 3c

entries	monomer	solvent	[monomer] (mol L^{-1})	time (h)	yield (%)	$M_n \times 10^{-6}$	DP$_n$[c]	PDI	LCST (°C)
			polymerization conditions[a]			GPC results[b]			
1[d]	**2c**	DMF	1.06	7.0	55	0.48	720	2.54	63.2
2[e]	**2c**	Water	0.48	15.0	60	2.00	3020	2.48	63.0
3[d]	**2c**	Bulk	1.66[f]	4.5	74	2.36	3560	4.92	62.6
4[e]	**3c**	Water	0.30	15.0	63	0.82	350	2.49	63.6
5[d]	**3c**	Bulk	0.47[f]	14.0	65	0.71	300	2.55	64.4

[a] All polymerizations were carried out at 60 °C. [b] All GPC measurements were done with DMF (1% LiBr) as eluent at 45 °C. [c] DP$_n$ = number-average degree of polymerization. [d] AIBN as initiator with a concentration of 0.5 wt % based on monomer. [e] ACVA as initiator with a concentration of 0.5 wt % based on monomer. [f] The values were obtained taking the monomer densities into account, which were determined to be 1.1 g mL^{-1} for both **2c** and **3c**.

resulting precipitate was filtered and THF evaporated. The residue was dissolved in DCM and washed with brine. After drying over MgSO$_4$, purification by column chromatography with DCM/MeOH (20:1, v/v) afforded **2b** (28.70 g, 93%) as a colorless oil. ^{1}H NMR (D$_2$O): δ 3.33 (s, 6H, CH$_3$), 3.35 (s, 3H, CH$_3$), 3.53−3.59 (m, 6H, CH$_2$), 3.63−3.68 (m, 12H, CH$_2$), 3.71 (t, 2H, CH$_2$), 3.74 (t, 4H, CH$_2$), 3.82 (t, 2H, CH$_2$), 3.90 (t, 4H, CH$_2$), 4.17 (t, 2H, CH$_2$), 4.22 (t, 4H, CH$_2$), 4.55 (s, 2H, CH$_2$), 6.75 (s, 2H, CH). ^{13}C NMR (D$_2$O): δ 58.13, 63.79, 68.30, 69.33, 69.58, 69.60, 69.63, 69.75, 69.80, 69.92, 70.21, 71.12, 72.14, 106.45, 135.96, 137.29, 151.99. HR-MS: *m/z* calcd, 617.33; found, 617.3150 [M + Na]$^+$.

3,4,5-Tris(2-(2-(2-methoxyethoxy)ethoxy)ethoxy)benzyl methacrylate (2c). Methacryloyl chloride (MAC) (0.70 g, 6.72 mmol) was added dropwise to a mixture of **2b** (2.00 g, 3.36 mmol), TEA (1.70 g, 16.80 mmol), and DMAP (0.10 g) in dry DCM at 0 °C over 5 min. The mixture was stirred for 3 h at r.t. After being successively washed with aqueous NaHCO$_3$ solution and brine, the organic phase was dried over MgSO$_4$. Purification by column chromatography with DCM/MeOH (20:1, v/v) afforded **2c** (2.00 g, 90%) as a colorless oil. ^{1}H NMR (D$_2$O): δ 1.88 (s, 3H,CH$_3$), 3.32 (s, 6H, CH$_3$), 3.34 (s, 3H, CH$_3$), 3.53−3.55 (m, 4H, CH$_2$), 3.56−3.58 (m, 2H, CH$_2$), 3.61−3.66 (m, 12H, CH$_2$), 3.67−3.69 (m, 2H, CH$_2$), 3.71−3.73 (m, 4H, CH$_2$), 3.81 (t, 2H, CH$_2$), 3.87 (t, 4H, CH$_2$), 4.16−4.18 (m, 6H, CH$_2$), 5.08 (s, 1H, CH$_2$), 5.69 (s, 1H, CH$_2$), 6.10 (s, 1H, CH$_2$), 6.75 (s, 2H, CH). ^{13}C NMR (D$_2$O): δ 17.53, 58.13, 66.78, 68.34, 69.27, 69.60, 69.66, 69.78, 69.98, 70.22, 71.13, 72.12, 107.35, 127.20, 132.41, 135.85, 136.69, 152.09, 169.18. HR-MS: *m/z* calcd, 685.35; found, 685.3397 [M + Na]$^+$.

3,4,5-Tris(2-(2-(2-(3,4,5-tris(2-(2-(2-methoxyethoxy)ethoxy)etho-xy)benzyl-oxy)ethoxy)ethoxy)ethoxy)benzoic acid (3a). Compound **2d** (5.30 g, 5.08 mmol) in dry THF (50 mL) was added dropwise to a mixture of **2b** (10.00 g, 16.76 mmol), KI (0.49 g, 3.05 mmol), 15-crown-5 (3.69 g, 16.76 mmol), and NaH (1.21 g, 50.29 mmol) in dry THF (100 mL). The mixture was stirred for 24 h at r.t. before addition of MeOH to quench the excess NaH. After evaporation of solvent in vacuo, the residue was dissolved in DCM and successively washed with aqueous NaHCO$_3$ and brine. After drying over MgSO$_4$, purification by column chromatography with DCM/MeOH (15:1, v/v) afforded **3a** (5.20 g, 44%) as a yellow oil. ^{1}H NMR (D$_2$O): δ 3.31 (s, 18H, CH$_3$), 3.34 (s, 9H, CH$_3$), 3.54 − 3.69 (m, 96H, CH$_2$), 3.79 − 3.82 (m, 24H, CH$_2$), 4.10−4.12 (m, 24H, CH$_2$), 4.40 (s, 4H, CH$_2$), 4.43 (s, 2H, CH$_2$), 6.64 (s, 4H, CH), 6.68 (s, 2H, CH), 7.21 (s, 2H, CH). ^{13}C NMR (D$_2$O): δ 58.16, 58.18, 68.25, 68.57, 69.07, 69.29, 69.61, 69.63, 69.68, 69.77, 69.81, 69.88, 69.97, 70.17, 70.31, 71.15, 72.17, 72.35, 72.65, 106.97, 107.01, 108.63, 125.61, 134.28, 134.36, 136.19, 141.36, 151.87, 151.97, 152.00, 169.11. HR-MS: *m/z* calcd, 2319.20; found, 2319.179 [M + Na]$^+$.

3,4,5-Tris(2-(2-(2-(3,4,5-tris(2-(2-(2-methoxyethoxy)ethoxy)etho-xy)benzyl-oxy)ethoxy)ethoxy)ethoxy)benzyl alcohol (3b). N-Methylmorpholine (0.65 g, 6.44 mmol) and ethyl chloroformate (0.70 g, 6.44 mmol) were added sequentially to a solution of **3a** (3.70 g, 1.61 mmol) in dry THF (80 mL) at −15 °C, and the mixture was stirred for 1 h. NaBH$_4$ (0.49 g, 12.88 mmol) was then added at −5 °C and the reaction mixture was stirred for another 2 h. Water was added to quench the reaction and THF then evaporated. The residue was dissolved in DCM and then washed successively with aqueous NaHCO$_3$ and brine. After drying over MgSO$_4$, purification by column chromatography with DCM/MeOH (15:1, v/v) afforded **3b**

(3 g, 82%) as a colorless oil. ^{1}H NMR (CD$_2$Cl$_2$): δ 3.33 (s, 27H, CH$_3$), 3.50 − 3.69 (m, 96H, CH$_2$), 3.76 (t, 8H, CH$_2$), 3.80−3.83 (m, 16H, CH$_2$), 4.10 (t, 8H, CH$_2$), 4.12−4.14 (m, 16H, CH$_2$), 4.44 (s, 6H, CH$_2$), 4.54 (s, 2H, CH$_2$), 6.60 (s, 6H, CH), 6.62 (s, 2H, CH). ^{13}C NMR (CD$_2$Cl$_2$): δ 58.98, 65.20, 69.03, 69.89, 70.07, 70.14, 70.76, 70.77, 70.79, 70.90, 70.92, 70.97, 71.09, 72.27, 72.65, 73.41, 77.47, 106.24, 106.29, 107.04, 127.20, 134.44, 137.57, 137.81, 152.93, 152.99. HR-MS: *m/z* calcd, 2305.23; found, 2305.206 [M + Na]$^+$.

3,4,5-Tris(2-(2-(2-(3,4,5-tris(2-(2-(2-methoxyethoxy)ethoxy)etho-xy)benzyl-oxy)ethoxy)ethoxy)ethoxy)benzyl methacrylate (3c). MAC (0.55 g, 5.26 mmol) was added dropwise to a mixture of **3b** (2.40 g, 1.05 mmol), TEA (0.53 g, 5.26 mmol), and DMAP (0.1 g) in dry DCM (50 mL) at 0 °C over 5 min. The mixture was stirred for 5 h at r.t. and then quenched with MeOH. After being washed successively with aqueous NaHCO$_3$ solution and brine, the organic phase was dried over MgSO$_4$. Purification by column chromatography with DCM/MeOH (20:1, v/v) afforded **3c** (2.16 g, 88%) as a colorless oil. ^{1}H NMR (CD$_2$Cl$_2$): δ 1.99 (s, 3H, CH$_3$), 3.36 (s, 18H, CH$_3$), 3.37 (s, 9H, CH$_3$), 3.53−3.55 (m, 18H, CH$_2$), 3.62 − 3.73 (m, 78H, CH$_2$), 3.79 (t, 8H, CH$_2$), 3.86−3.87 (m, 16H, CH$_2$), 4.13−4.18 (m, 24H, CH$_2$), 4.47 (s, 6H, CH$_2$), 5.11 (s, 2H, CH$_2$), 5.63 (s, 1H, CH$_2$), 6.16 (s, 1H, CH$_2$), 6.63 (s, 6H, CH), 6.67 (s, 2H, CH). ^{13}C NMR (CD$_2$Cl$_2$): δ 18.25, 58.74, 66.45, 68.82, 68.89, 69.66, 69.84, 70.55, 70.57, 70.67, 70.70, 70.87, 72.04, 72.43, 72.46, 73.19, 106.83, 107.49, 125.55, 134.18, 136.55, 137.63, 138.21, 152.71, 152.79, 167.08. HR-MS: *m/z* calcd, 2373.25; found, 2373.243 [M + Na]$^+$.

General Procedure for Polymerization in DMF Solution (A). The required amounts of monomer and AIBN (0.5 wt % to the monomer) were dissolved in DMF in a Schlenk tube. The solution was thoroughly deoxygenated by several freeze−pump−thaw cycles and then stirred at 60 °C for the designed time. After cooling to r.t., the polymer was dissolved in DCM and purified by silica gel column chromatography with DCM as eluent.

General Procedure for Polymerization in Aqueous Solution (B). The required amounts of monomer and 4,4′-azobis(4-cyanovaleric acid) (ACVA; 0.5 wt % to the monomer) were dissolved in water inside a Schlenk tube. The solution was thoroughly deoxygenated by several freeze−pump−thaw cycles and then stirred at 60 °C for designed time. The purification of the polymer followed the same process as in procedure **A**.

General Procedure for Polymerization in Bulk (C). The required amounts of monomer and AIBN (0.5 wt % to the monomer) were added into a Schlenk tube. The mixture was thoroughly deoxygenated by several freeze−pump−thaw cycles and then stirred at 60 °C for the designed time. The purification of the polymer followed the same process as in procedure **A**.

Poly(3,4,5-tris(2-(2-(2-methoxyethoxy)ethoxy)ethoxy)benzyl meth-acrylate) (PG1). Route 1: According to general procedure **A** from **2c** (0.40 g, 0.60 mmol), AIBN (2.0 mg), and DMF (0.2 mL), polymerization for 7 h yielded **PG1** as a colorless gel (0.22 g, 55%). ^{1}H NMR (CD$_2$Cl$_2$): δ 0.86−1.09 (m, 3H, CH$_3$), 1.90−2.05 (m, 2H, CH$_2$), 3.29−3.31 (m, 9H, CH$_3$), 3.46−3.64 (m, 24H, CH$_2$), 3.74 (br, 6H, CH$_2$), 4.06 (br, 6H, CH$_2$), 4.81 (br, 2H, CH$_2$), 6.54 (br, 2H, CH). ^{13}C NMR (CD$_2$Cl$_2$): δ 58.68, 68.91, 69.76, 70.50, 72.03, 72.50, 107.12, 130.87, 138.13, 152.83. The signals from the polymer backbone were so broad that they disappeared in the baseline. Elemental analysis (%) calcd for (C$_{32}$H$_{54}$O$_{14}$)$_n$ (662.77)$_n$: C, 57.99;

Scheme 1. Synthesis Procedures for G1 and G2 Macromonomers 2c and 3c
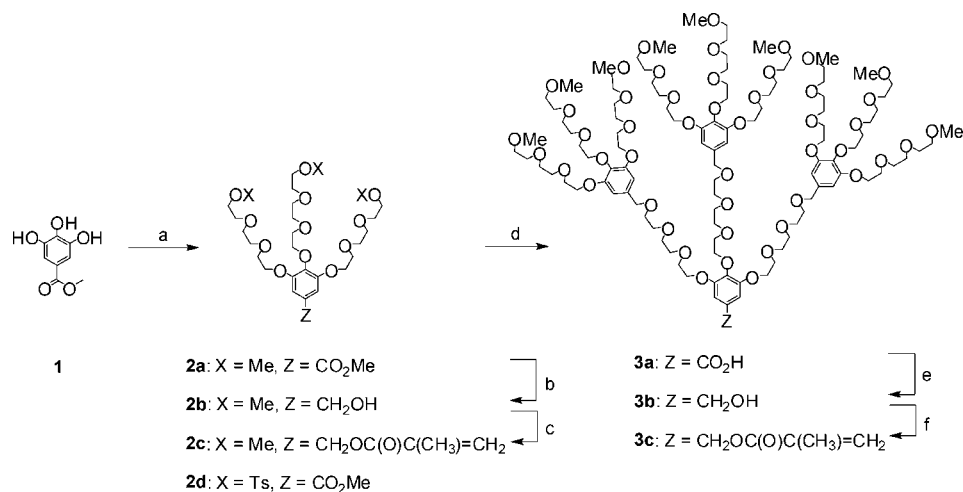
Reagents and conditions: (a) Me-TEG-Ts, K$_2$CO$_3$, KI, DMF, 80 °C, 24 h (94%); (b) LAH, THF, −5 to 25 °C, 3 h (93%); (c) MAC, TEA, DMAP, DCM, 0−25 °C, 3 h (90%); (d) KI, 15-crown-5, NaH, THF, r.t., 24 h (44%); (e) (i) *N*-methylmorpholine, ethyl chloroformate, THF, −15 °C, 1 h; (ii) NaBH$_4$, −5°C, 2 h (82%); (f) MAC, TEA, DMAP, DCM, 0−25 °C, 5 h (88%).

H, 8.21. Found: C, 57.27; H, 8.22. Route 2: According to general procedure **B** from **2c** (0.50 g, 0.75 mmol), ACVA (3.6 mg), and pure water (1.11 mL), polymerization for 15 h yielded **PG1** as a colorless gel (0.30 g, 60%). The identical spectral data as in route 1 were obtained. Route 3: According to general procedure **C** from **2c** (3.2 g, 4.8 mmol) and AIBN (16 mg), polymerization for 4.5 h yielded **PG1** as a colorless gel (2.38 g, 74%). The identical spectral data as in route 1 were obtained.

Poly(3,4,5-tris(2-(2-(2-(3,4,5-tris(2-(2-(2-methoxyethoxy)ethoxy)ethoxy)ethoxy) benzyloxy)ethoxy)ethoxy)ethoxy)benzyl methacrylate) (PG2). Route 1: According to general procedure **B** from **3c** (0.40 g, 0.17 mmol), ACVA (2.8 mg), and pure water (0.2 mL), polymerization for 15 h yielded **PG2** as a colorless gel (0.25 g, 63%). ^{1}H NMR (CD$_2$Cl$_2$): δ 3.30−3.37 (m, 27H, CH$_3$), 3.46−3.66 (m, 96H, CH$_2$), 3.78 (br, 24H, CH$_2$), 4.08 (br, 24H, CH$_2$), 4.40 (br, 6H, CH$_2$), 6.53−6.56 (br, 8H, CH). ^{13}C NMR (CD$_2$Cl$_2$): δ 58.71, 68.84, 69.67, 69.79, 70.48, 70.61, 70.80, 72.00, 72.44, 73.09, 106.52, 134.14, 137.54, 152.70. The signals from the polymer backbone were so broad that they disappeared in the baseline. Elemental analysis (%) calcd for (C$_{113}$H$_{192}$O$_{50}$)$_n$ (2350.73)$_n$: C, 57.74; H, 8.23. Found: C, 57.46; H, 8.25. Route 2: According to general procedure **C** from **2c** (0.4 g, 0.17 mmol) and AIBN (2 mg), polymerization for 14 h yielded **PG2** as colorless gel (0.26 g, 65%). The identical spectral data as in route 1 were obtained.

Results and Discussion

Synthesis and Characterization. The synthesis of all dendrons and macromonomers followed a procedure similar to the one in a previous report (Scheme 1).[15] Starting from methyl gallate, Williamson etherification with Me-TEG-Ts afforded the corresponding branching unit **2a**, which was reduced with LAH to alcohol **2b**. This alcohol was then transferred into G1 macromonomer **2c** by reaction with methacryloyl chloride (MAC). The corresponding G2 macromonomer **3c** was synthesized in three steps. Etherification of the tosylate **2d** with alcohol **2b** directly gave acid **3a**, whose reduction to alcohol **3b** was achieved according to Kokotos' protocol.[17] This alcohol was then esterified with MAC to furnish **3c**. Both macromonomers **2c** and **3c** were obtained on a gram scale as completely colorless, water-soluble liquids whose fluidity is reminiscent of glycerol. After column chromatography, the yields amounted to 79 and 33%, respectively, based on branching unit **2a**. It should be noted that the dendritic macromonomers developed so far by the authors' laboratory are practically all solids. Normally solid materials are preferred for ease of purification; however, when

it comes to polymerization, specifically if high molar mass monomers are concerned, their maximally realizable concentration is critical to achieving high degree of polymerization products. Liquid monomers, though more tedious to purify, can have a considerable advantage here, because either more highly concentrated solutions can be prepared or the polymerizations can even be conducted in bulk. These concentration effects were first described by Tsukahara and are typical for what is commonly referred to as "macromonomers".[18]

The free radical polymerizations of macromonomers **2c** and **3c** were carried out in water and bulk. The polymerization of **2c** was additionally carried out in DMF solution aiming at a somewhat lower molar mass product for the subsequent studies on its aggregation behavior in aqueous solution. All polymerizations were conducted at 60 °C. The polymers were obtained in yields of 55−74% after purification by silica gel column chromatography. It should be noted here that for the polymerization of **2c** in water, the polymerization solution was clear at the beginning and turned turbid at a later stage. The molar masses were determined by gel permeation chromatography (DMF with 1% LiBr, 45 °C, 2 angle light scattering detection) based on monomodal elution curves. The results are compiled in Table 1 and leads to the following conclusions: (1) The number average degree of polymerization (DP$_n$) for **PG1** obtained in water (entry 2) is larger than in DMF (entry 1), although the monomer concentration was lower in the former than in latter case. (2) Bulk polymerization (entry 3) gave the highest molar mass for **PG1** in the shortest time. (3) The DP$_n$ values for **PG2** are lower by roughly a factor of 10 than those for **PG1** although comparable monomer concentrations were applied (entries 2 and 5). Steric hindrance seems to be responsible for this. Further, not much difference is observed whether the polymerizations of **3c** are carried out in bulk or in concentrated aqueous solutions (entries 4 and 5).

The dendronized polymers **PG1** and **PG2** are highly soluble in conventional organic solvents, such as THF, dichloromethane, and chloroform, as well as in water, and have glass-transition temperatures (T_g) below −80 °C, which is much lower than those of the closely related polymers **PG1(OH)** (T_g = −45 °C) and **PG2(OH)** (T_g = −40 °C).[15] The ^{1}H NMR spectra of **PG1** (Table 1, entry 2) were recorded in CD$_2$Cl$_2$ and D$_2$O and are shown in Figure 2 with full signal assignment. In CD$_2$Cl$_2$ (Figure 2a), most proton signals from dendron (g−j, k) appear sharp, whereas some proton signals from dendron (c−f) and backbone
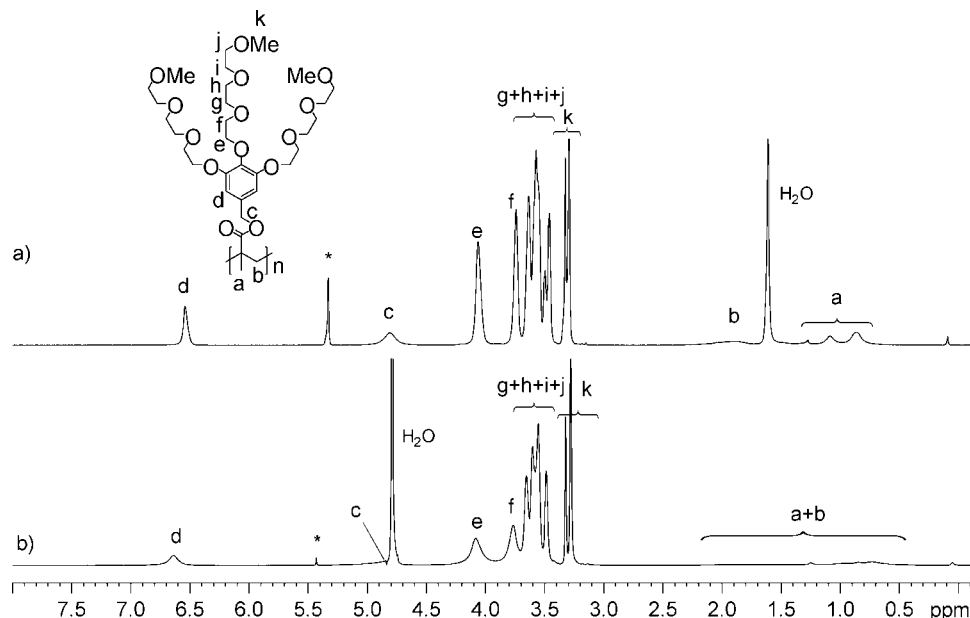
Figure 2. ^{1}H NMR spectra of **PG1** (Table 1, entry 2; 4.0 wt %) in (a) CD$_2$Cl$_2$ and (b) in D$_2$O at room temperature.
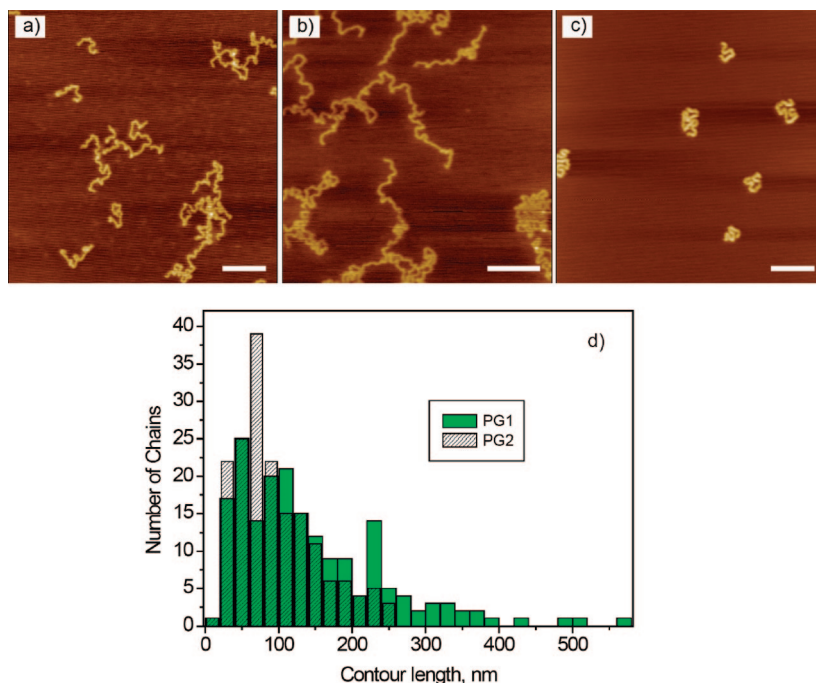

Figure 3. Tapping mode AFM images of (a) **PG1** (Table 1, entry 1), (b) **PG1** (Table 1, entry 2), and (c) **PG2** (Table 1, entry 5) on mica; (d) the contour length distributions of **PG1** and **PG2**. The scale bars in a−c are the same and correspond to 100 nm. The Z scale is 2 nm for **PG1** (a, b) and 4 nm for **PG2** (c). Samples were prepared from chloroform solutions (3 mg/L for **PG1** and 4 mg/L for **PG2**) by spin coating (2000 rpm).

(a, b) are slightly broadened. Rather different results were observed in D$_2$O (Figure 2b). Even more signals from protons close to and from the backbone are very broad now or even disappear. This indicates that in aqueous medium the backbone is less flexible which may be the result of some compression in an attempt to protect itself against water. The ^{1}H NMR spectra of **PG2** were also recorded in both solvents (see the Supporting Information). Unfortunately the spectrum obtained in D$_2$O exhibits only very broad and unstructured signals, rendering a comparison not practical.

The polymers **PG1** and **PG2** were also investigated by atomic force microscopy (AFM) when spin-coated on mica to prove their linearity and to arrive at independent molar mass data based on histographic contour lengths analysis. Figure 3 shows typical

images for both polymers with well-resolved chains exhibiting homogeneous apparent heights and widths and a negligible indication of branching if there is any such structural mistake. **PG1** of slightly lower molar mass (Table 1, entry 1) was used for the contour length analysis (Figure 3a). For this purpose, 187 individual chains were selected and provided an average contour length of 142 nm (Figure 3d). Given the respective experimental limitations of AFM and GPC this value agrees well with the GPC result (DP$_n$ = 720), which translates into a contour length of 180 nm in the fully stretched conformation. For **PG1** of high molar mass (Table 1, entry 2), the chains are so long that they are partially involved in aggregates despite the rather low concentration of 3 mg/L used for sample preparation (Figure 3b). This sample could therefore not be used
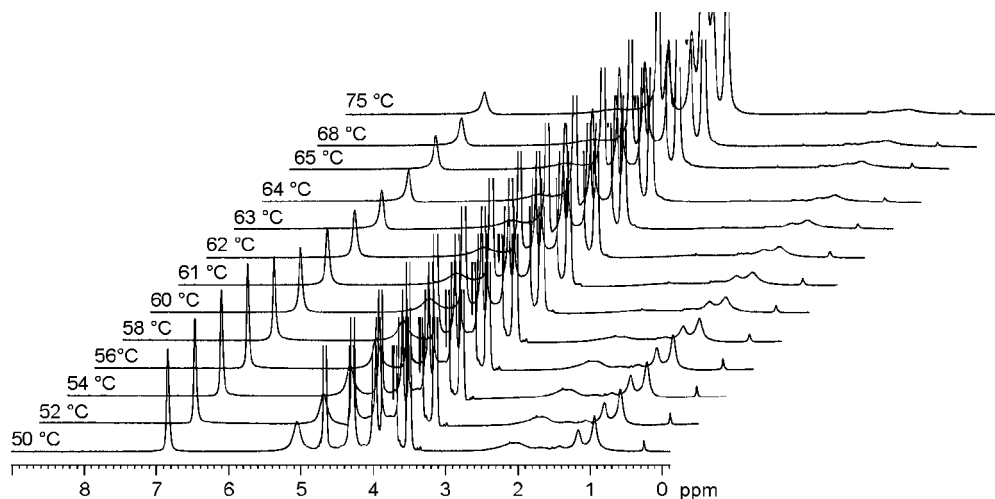
Figure 4. Temperature-dependent ^{1}H NMR spectra of **PG1** (Table 1, entry 2; 2.0 wt %) in D_2O.
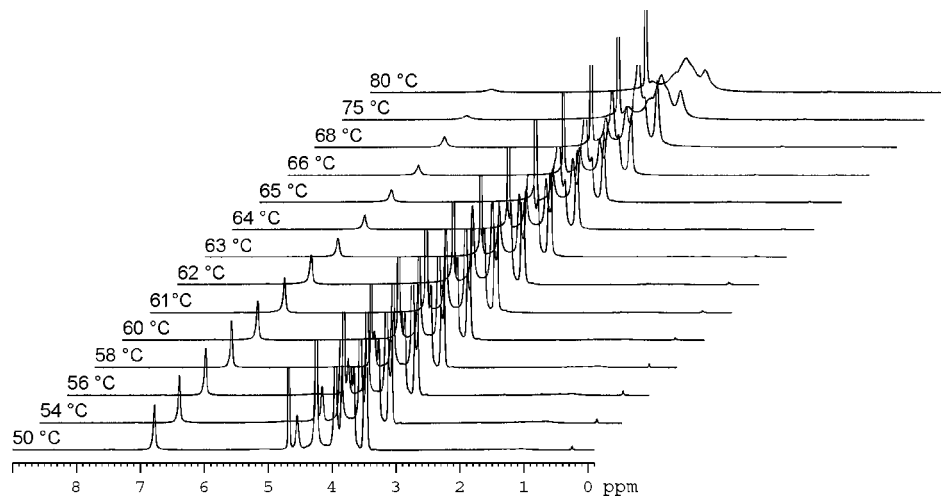
Figure 5. Temperature-dependent ^{1}H NMR spectra of **PG2** (Table 1, entry 5; 2.0 wt %) in D_2O.

for contour length analysis. For **PG2**, the chains are shorter and well-separated from one another (Figure 3c) so that 174 individual chains could be selected, which provided an average contour length of 96 nm. This value is again in the same order of magnitude as the GPC result of $DP_n = 300$, which translates into a contour length of 75 nm in the fully stretched conformation.

Thermoresponsive Behavior. The dehydration process of both polymers was first investigated by ^{1}H NMR spectroscopy. The corresponding spectra of **PG1** and **PG2** are shown in Figures 4 and 5 for the temperature ranges of 50−75 and 50−80 °C, respectively. As the temperature increased above approximately 58 and 62 °C for **PG1** and **PG2**, respectively, the signals at 0.75−1.30, 1.80−2.20, 3.74, 4.06, and 6.52 ppm became increasingly broader and their heights decreased. This phenomenon is typically interpreted in terms of dehydration of the OEG chains,[19] and the corresponding temperatures are closely related to the polymers' LCSTs. Taking **PG1** (Table 1, entry 2) as an example, the broadening started between 58 and 60 °C irrespective of whether low (0.5 wt %) or high (4.0 wt %) concentrations were used (see Figure S1 in the Supporting Information for the corresponding ^{1}H NMR spectra). These temperatures, though not resembling LCSTs, are much lower than the LCSTs for linear PEGs which are in the range of 100−176 °C depending on molar mass.[20]

Turbidity measurements using UV/vis spectroscopy aiming at a LCST determination[3] were performed for all samples listed in Table 1, in order to see whether there are molar mass and/or generation dependencies (for the actual values, consult Table 1). Representative plots of transmittance versus temperature during heating and cooling for two samples of **PG1** and one sample of **PG2** are shown in Figure 6a (For others refer to Figure S2 in the Supporting Information). Three features of these curves should be pointed out: (1) The transmittance below all LCSTs is close to 100%, whereas that above is close to zero. This suggests that for the concentrations used, the polymer solutions are fully transparent below LCST, while aggregates are formed above this transition, which are large and compact[21] enough to scatter light efficiently. (2) The transitions are sharp in both heating and cooling directions. The temperature difference between on- and off-set of the heating and cooling curves at the transition is less than 1 ° for all samples. Whereas the heating curve is similar to that of P*N*iPAM, the cooling curve is much sharper than that of this important reference material[22] and also of grafted OEG copolymers.[9] (3) The hystereses span less than 0.5 °C for both **PG1** and **PG2**. The sharpness of the phase transition is related to the width of the corresponding phase diagram's unstable regime. Presently we are in the process of measuring these diagrams. In addition, the aggregation and deaggregation processes are fast. Upon immersing a solution of any of the polymers in a thin-walled NMR tube into a preheated bath at 65 °C, the clear solution turns turbid in a few seconds and the reverse process gives a clear solution also in the same time range. The fast dehydration and especially the
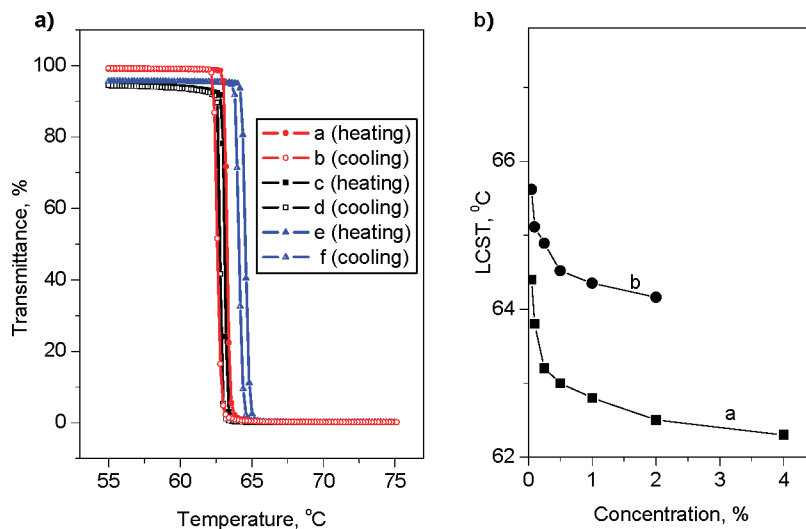
Figure 6. (a) Plots of transmittance vs temperature for 0.25 wt % aqueous solutions of **PG1** and **PG2**. Heating and cooling rate = 0.2 °C/min. Curves a and b, **PG1** (Table 1, entry 1); curves c and d, **PG1** (Table 1, entry 2); curves e and f, **PG2** (Table 1, entry 5). (b) Dependence of LCSTs on polymer concentrations. Curve a, **PG1** (Table 1, entry 2), and curve b, **PG2** (Table 1, entry 5). Detailed plots of transmittance vs temperature for different polymer concentrations are shown in Figure S3 in the Supporting Information.

fast rehydration may be a result of the high packing density of OEG chains which renders the transition dependent on the out- and influx of a small number of water molecules only. This argumentation is supported by the fact that the DSC analysis shows the transition at LCST not to be associated with a sizable enthalpy. For a recent interpretation on the factors that influence the kinetics of aggregation processes of thermoresponsive polymers, see ref.[7b] The LCST values of **PG1** (Table 1, entry 2) and **PG2** (Table 1, entry 5) are 63.0 and 64.4 °C, respectively. These data are close to those obtained from the temperature-dependent proton NMR measurements, which suggests the polymer aggregation to virtually start simultaneously with the chain dehydration. The molar mass dependence of the phase transitions was examined for **PG1** and found to be negligible in the range investigated (see Table 1). The simplest interpretation is that even the short chains are already long enough to show a molar-independent and thus polymer-typical effect. The concentration dependence was investigated for both **PG1** and **PG2**. Their LCST values decreased with increasing concentration from 0.05 to 4.0 wt % (Figure 6b) with the total effects being small (within 2°). Next, the effect of architecture on LCST was looked into qualitatively. The LCST of a polymer depends mostly on the hydrophilicity−hydrophobicity balance with the more hydrophilic polymers commonly showing higher LCSTs than the more hydrophobic ones. According to an often applied increment method to quantify hydrophilicity (log P, where P = [solute]$_{\text{n-octanol}}$/[solute]$_{\text{water}}$),[6] the corresponding value (based on each repeat unit) for **PG1** is log P = 0.35. For a closely related comb polymethacrylate derivative, which carries a single straight methoxy end-capped TEG side chain in each repeat unit,[8c] this value is log P = 0.32. Though both values are close to one another, the LCST of the latter polymer is 10° lower and the thermal transition spans a broader range (47−53 °C) than **PG1**. That log P values alone are insufficient to predict LCSTs is shown even more clearly with the following **PG2** case. Its log P = −1.04, which is much lower than that of **PG1** and a significantly higher LCST for **PG2** would therefore be predicted. Because this is not the case (ΔLCST = 1.4 °), there seems to be a counter effect operative about whose nature one can only speculate at this point.[23]

Thermally Induced Aggregation. Based on the evidence from ^{1}H NMR spectroscopy and the turbidity measurements, polymers **PG1** and **PG2** undergo fully reversible aggregation around LCST. These processes were further investigated by

optical microscopy (OM) for direct visualization of the aggregate morphologies. Additionally, the aggregation and deaggregation were video-taped with a high-resolution CCD camera in time intervals of a second to gain a complete picture of all steps in these processes. For the corresponding high-resolution movies for **PG1** and **PG2**, the reader is referred to the Supporting Information. Some aspects will nevertheless be discussed here. **PG1** was used in relatively high concentration (0.25 wt %), whereas solutions of **PG2** had two different concentrations (0.05 and 0.25 wt %) in order to check whether the aggregate morphologies are concentration dependent. All OM images were fully reproducible, and representative ones are shown in Figure 7. Below LCST no aggregates were visible for both polymers (Figure 7a). Above LCST, aggregates from **PG1** and **PG2** were observed which differed in their morphology. For **PG1** at 63 °C irregular aggregates formed, which at 64 °C changed into complex, larger ones (images b and c in Figure 7). Upon cooling back to 63 °C, different morphologies were observed, indicating pronounced hystereses (Figure 7d; also see video). All aggregates disappeared again when the temperature dropped to 62 °C (Figure 7a). In contrast, **PG2** behaved quite differently. Above LCST, uniform spherical aggregates (images e and f in Figure 7) with diameters around 1−3 μm (see inset in images e and f, Figure 7) were always observed for both concentrations. They appear to be the same regardless of whether a cooling or heating process is monitored. The concentrations applied here showed negligible influence on the aggregation process as well as both aggregate size and morphology (compare image e with image f in Figure 7).

The large aggregate sizes of **PG1** and **PG2** and specifically the fact that **PG2** forms more or less uniform objects that do not grow upon slight temperature change are not understood yet. It is to be expected that upon dehydration, the persistence lengths of **PG1** and **PG2** increase and that it may be justified to consider them as rigid rods. It should, however, be stressed that rigidity is by far not the only factor that influences aggregate size. Surface tension, polarization effects, surface charges, and the like would also have to be considered.

Conclusion and Outlook

The efficient syntheses of two structurally novel thermoresponsive polymers using the structure principles of dendronized polymers (**PG1** and **PG2**) were described. In contrast to most other dendritic macromolecules with this property, the thermo-
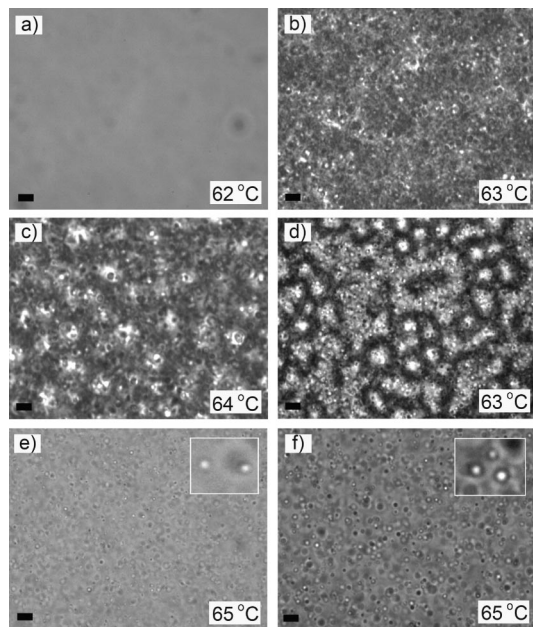
Figure 7. Optical micrograph of the aggregates from aqueous solutions of **PG1** (Table 1, entry 2) and **PG2** (Table 1, entry 5). All images have the same scale bar of 10 μm. (a) **PG1** (0.25 wt %), after heating to 62 °C (some dust particles to be seen); **PG1** (0.25 wt %), after further heating to (b) 63 and (c) to 64 °C; (d) the same sample after cooling to 63 °C; (e) **PG2** (0.05 wt %), 65 °C; (f) **PG2** (0.25 wt %), 65 °C. Images e and f contain inserts with 4 times enlarged features. Note that the white features are the ones in focus.

responsive nature of these dendronized polymers may result from the entire branch-work and not from just a peripheral decoration. The observed transitions are fully reversible upon both heating and cooling and sharper than those published for other polymers.[8–11] This behavior can not only be explained in terms of their hydrophilicity−hydrophobicity balance, but similar to spherical dendrimers, there seems to be a significant contribution resulting from the concrete structural arrangement of hydrophilic and hydrophobic units. The aggregation process was monitored by OM and corresponding high-resolution videos are provided. According to these OM images, **PG2** forms uniform spherical aggregates with sizes in the range of a few micrometers which are always observed above LCST irrespective of whether the samples are in a heating or cooling process. The uniformity of the **PG2** particles is also independent of heating rate and concentration. Obviously, there is no fast Ostwald ripening. In contrast, for **PG1** a more complex aggregation process leading to less defined aggregate morphologies is observed, which is also dependent on heating rate and concentration, and also differs for heating and cooling. It seems that **PG1** behaves more like a conventional thermoresponsive polymer than **PG2**. The processes involved in aggregate formation are presently under study. We would also like to point out that the polymer structures reported here may look rather complex compared to some other thermoresponsive polymers, the synthetic procedures developed here, however, allow to synthesize the G2 macromonomer on a few gram scale within 2 weeks and at low cost.

First orienting experiments show that only slight chemical changes at the periphery of the polymers (e.g., changing the methyl against an ethyl group) have a pronounced effect on LCST while keeping the sharpness of the transitions in both directions the same. We therefore believe we have a versatile and powerful system for various bio- and sensor applications at hand that spans a considerable temperature and application range.

Supporting Information Available: Temperature-dependent ^{1}H NMR spectra of **PG1** at different concentrations, ^{1}H and ^{13}C NMR spectra of all new compounds and polymers, plots of transmittance vs temperature for **PG1** and **PG2** at different concentrations (PDF); recorded optical microscopic movies (.AVI). This material is available free of charge via the Internet at http://pubs.acs.org.

References and Notes

(1) (a) Schild, H. G. *Prog. Polym. Sci.* **1992**, *17*, 163–249. (b) Gil, E. S.; Hudson, S, M. *Prog. Polym. Sci.* **2004**, *29*, 1173–1222. (c) Alarcon, C. H.; Pennadam, S.; Alexander, C. *Chem. Soc. Rev.* **2005**, *34*, 276–285. (d) Yerushalmi, R.; Scherz, A.; van der Boom, M. E.; Kraatz, H.-B. *J. Mater. Chem.* **2005**, *15*, 4480–4487. (e) Kumar, A.; Srivastava, A.; Galaev, I. Y.; Mattiasson, B. *Prog. Polym. Sci.* **2007**, *32*, 1205–1237.

(2) (a) Schmaljohann, D. *Adv. Drug Delivery Rev.* **2006**, *58*, 1655–1670. (b) Hoffman, A. S.; Stayton, P. S. *Prog. Polym. Sci.* **2007**, *32*, 922–932. (c) Duncan, R. *Nat. Rev. Drug Discovery* **2003**, *2*, 347–360. (d) Tao, L.; Mantovani, G.; Lecolley, F.; Haddleton, D. M. *J. Am. Chem. Soc.* **2004**, *126*, 13220–13221. (e) Ma, H.; Hyun, J.; Stiller, P.; Chilkoti, A. *Adv. Mater.* **2004**, *16*, 338–341. (f) Popescu, D. C.; Lems, R.; Rossi, N. A. A.; Yeoh, C.-T.; Loos, J.; Holder, S. J.; Bouten, C. V. C.; Sommerdijk, N. A. J. M. *Adv. Mater.* **2005**, *17*, 2324–2329.

(3) Precisely speaking, this transition temperature should be referred to as lower critical aggregation temperature (LCAT) because this term describes more precisely the effect that is observed by turbidity measurements (cloud point determinations). Though strictly speaking the term LCST is wrong in the present connection, it is nevertheless much more often used than LCAT, and we will therefore stick to it throughout the manuscript.

(4) (a) For example, see Gillies, E. R.; Jonsson, T. B.; Fréchet, J. M. J. *J. Am. Chem. Soc.* **2004**, *126*, 11936–11943. (b) Sosnic, A.; Cohn, D. *Biomaterials* **2005**, *26*, 349–357. (c) Convertine, A. J.; Lokitz, B. S.; Vasileva, Y.; Myrick, L. J.; Scales, C. W.; Lowe, A. B.; McCormick, C. L. *Macromolecules* **2006**, *39*, 1724–1730. (d) Li, Y.; Lokitz, B. S.; McCormick, C. L. *Angew. Chem., Int. Ed.* **2006**, *45*, 5792–5795. (e) Cheng, C.; Schmidt, M.; Zhang, A.; Schlüter, A. D. *Macromolecules* **2007**, *40*, 220–227. (f) Sinturel, C.; Vayer, M.; Erre, R.; Amenitsch, H. *Macromolecules* **2007**, *40*, 2532–2538. (g) Xiao, X.; Fu, Y.-Q.; Zhou, J.-J.; Bo, Z.-S.; Li, L.; Chan, C.-M. *Macromol. Rapid Commun.* **2007**, *28*, 1003–1009. (h) Zhang, X.; Li, J.; Li, W.; Zhang, A. *Biomacromolecules* **2007**, *8*, 3557–3567.

(5) (a) Chen, G.; Hoffman, A. S. *Nature* **1995**, *373*, 49–52. (b) Lin, H.-H.; Cheng, Y.-L. *Macromolecules* **2001**, *34*, 3710–3715. (c) Li, C.; Gunari, N.; Fischer, K.; Janshoff, A.; Schmidt, M. *Angew. Chem., Int. Ed.* **2004**, *43*, 1101–1104. (d) Gunari, N.; Schmidt, M.; Janshoff, A. *Macromolecules* **2006**, *39*, 2219–2224. (e) Plummer, R.; Hill, D. J. T.; Whittaker, A. K. *Macromolecules* **2006**, *39*, 8379–8388.

(6) Viswanadhan, V. N.; Ghose, A. K.; Revankar, G. R.; Robins, R. K. *J. Chem. Inf. Comput. Sci.* **1989**, *29*, 163–172.

(7) (a) Jun, Y. J.; Toti, U. S.; Kim, H. Y.; Yu, J. Y.; Jeong, B.; Jun, M. J.; Sohn, Y. S. *Angew. Chem., Int. Ed.* **2006**, *45*, 6173–6176. (b) Van Durme, K.; Van Assche, G.; Aseyev, V.; Raula, J.; Tenhu, H.; Van Mele, B. *Macromolecules* **2007**, *40*, 3765–3772.

(8) (a) Allcock, H. R.; Pucher, S. R.; Turner, M. L.; Fitzpatrick, R. J. *Macromolecules* **1992**, *25*, 5573–5577. (b) Allcock, H. R.; Dudley, G. K. *Macromolecules* **1996**, *29*, 1313–1319. (c) Han, S.; Hagiwara, M.; Ishizone, T. *Macromolecules* **2003**, *36*, 8312–8319. (d) Zhang, D.; Macias, C.; Ortiz, C. *Macromolecules* **2005**, *38*, 2530–2534. (e) Hua, F.; Jiang, X.; Li, D.; Zhao, B. *J. Polym. Sci., Part A: Polym. Chem.* **2006**, *44*, 2454–2467.

(9) (a) Lutz, J.-F.; Akdemir, O.; Hoth, A. *J. Am. Chem. Soc.* **2006**, *128*, 13046–13047. (b) Lutz, J.-F.; Hoth, A. *Macromolecules* **2006**, *39*, 893–896.

(10) (a) Gitsov, I.; Fréchet, J. M. J. *J. Am. Chem. Soc.* **1996**, *118*, 3785–3786 (b) Kimura, M.; Kato, M.; Muto, T.; Hanabusa, K.; Shirai, H. *Macromolecules* **2000**, *33*, 1117–1119. (c) Kojima, C.; Haba, Y.; Fukui, T.; Kono, K.; Takagishi, T. *Macromolecules* **2003**, *36*, 2183–2186. (d) Haba, Y.; Harada, A.; Takagishi, T.; Kono, K. *J. Am. Chem. Soc.* **2004**, *126*, 12760–12761. (e) You, Y. Z.; Hong, C. Y.; Pan, C. Y.; Wang, P. H. *Adv. Mater.* **2004**, *16*, 1953–1957. (f) Gillies, E. R.; Jonsson, T. B.; Fréchet, J. M. J. *J. Am. Chem. Soc.* **2004**, *126*, 11936–11943. (g) Wan, D.; Fu, Q.; Huang, J. *J. Polym. Sci., Part A: Polym. Chem.* **2005**, *43*, 5652–5660. (h) Haba, Y.; Kojima, C.; Harada, A.; Kono, K. *Macromolecules* **2006**, *39*, 7451–7453. (i) Haba, Y.; Kojima, C; Harada, A; Kono, K. *Angew. Chem., Int. Ed.* **2007**, *46*, 234–237. (j) Zhou, Y.; Yan, D.; Dong, W.; Tian, Y. J. *Phys. Chem. B* **2007**, *111*, 1262–1270. (k) Chang, D. W.; Dai, L. *J. Mater. Chem.* **2007**, *17*, 364–371. (l) Liu, H.; Chen, Y.; Shen, Z. *J. Polym. Sci., Part A: Polym. Chem.* **2007**, *45*, 1177–1184.

(11) (a) Parrott, M. C.; Marchington, E. B.; Valliant, J. F.; Adronov, A. *J. Am. Chem. Soc.* **2005**, *127*, 12081–12089. (b) Aathimanikandan, S. V.; Savariar, E. N.; Thayumanavan, S. *J. Am. Chem. Soc.* **2005**, *127*, 14922–14929. (c) Jia, Z.; Chen, H.; Zhu, X.; Yan, D. *J. Am. Chem. Soc.* **2006**, *128*, 8144–8145. (d) Chen, H.; Jia, Z.; Yan, D.; Zhu, X. *Macromol. Chem. Phys.* **2007**, *208*, 1637–1645.

(12) (a) Schlüter, A. D.; Rabe, J. P. *Angew. Chem., Int. Ed.* **2000**, *39*, 864–883. (b) Zhang, A.; Shu, L.; Bo, Z.; Schlüter, A. D. *Macromol. Chem. Phys.* **2003**, *204*, 328–339. (c) Zhang, A. *Prog. Chem.* **2005**, *17*, 157–171. (d) Frauenrath, H. *Prog. Polym. Sci.* **2005**, *30*, 325–384. (e) Schlüter, A. D. *Top. Curr. Chem.* **2005**, *245*, 151–191.

(13) (a) For a few cases where micrometer-sized or even larger aggregates are formed, see for example: Jenekhe, S. A.; Chen, X. L. *Science* **1998**, *279*, 1903–1907. (b) Jenekhe, S. A.; Chen, X. L. *Science* **1999**, *283*, 372–375. (c) Yan, D.; Zhou, Y.; Hou, J. *Science* **2004**, *303*, 65–67. (d) Zhou, Y.; Yan, D. *Angew. Chem., Int. Ed.* **2005**, *44*, 3223–3226.

(e) Liu, C.; Gao, C.; Yan, D. *Angew. Chem., Int. Ed.* **2007**, *46*, 4128–4131.

(14) (a) Optical microscopy has been used for the observation of phase transition kinetics: Auernhammer, G. K.; Vollmer, D.; Vollmer, J. *J. Chem. Phys.* **2005**, *123*, 134511/1–134511/8. (b) For investigation of aggregate morphology but not their formation: Antonietti, M.; Förster, S. *Adv. Mater.* **2003**, *15*, 1323–1333. (c) Takakura, K.; Toyota, T.; Sugawara, T. *J. Am. Chem. Soc.* **2003**, *125*, 8134–8140. (d) Quemeneur, F.; Ramma, A.; Rinaudo, M.; Pépin-Donat, B. *Biomacromolecules* **2007**, *8*, 2512–2519.

(15) Li, W.; Zhang, A.; Schlüter, A. D. *Macromolecules* **2008**, *41*, 43–49.

(16) Ouchi, M.; Inoue, Y.; Liu, Y.; Nagamune, S.; Nakamura, S.; Wada, K.; Hakushi, T. *Bull. Chem. Soc. Jpn.* **1990**, *63*, 1260–1262.

(17) (a) Kokotos, G. *Synthesis* **1990**, 299–301. (b) Loukas, V.; Noula, C.; Kokotos, G. J. *Pept. Sci.* **2003**, *9*, 312–319.

(18) Tsukahara, Y.; Tsutsumi, K.; Okamoto, Y. *Makromol. Chem., Rapid Commun.* **1992**, *13*, 409–413.

(19) (a) Kjellander, R.; Florin, E. J. *Chem. Soc., Faraday Trans. 1* **1981**, *77*, 2053–2077. (b) Smith, G. D.; Bedrov, D. *J. Phys. Chem. B* **2003**, *107*, 3095–3097. (c) Ashbaugh, H. S.; Paulaitis, M. E. *Ind. Eng. Chem. Res.* **2006**, *45*, 5531–5537.

(20) Saeki, S.; Kuwahara, N.; Nakata, M.; Kaneko, M. *Polymer* **1976**, *17*, 685–689.

(21) Turbidity does not only depend on the size of the aggregates but also on the refractive index between aggregate and solvent.

(22) Wang, X.; Qiu, X.; Wu, C. *Macromolecules* **1998**, *31*, 2972–2976.

(23) (a) Fujishige, S.; Kubota, K.; Ando, I. *J. Phys. Chem.* **1989**, *93*, 3311–3313. (b) Djokpé, E.; Vogt, W. *Macromol. Chem. Phys.* **2001**, *202*, 750–757.

MA800129W